The Influence of Blue Light Exposure on Reconstructed 3-Dimensional Skin Model: Molecular Changes and Gene Expression Profile

Juliana Carvalhães Lago[1], Melissa Dibbernn Ganzerla[1], Ana Luisa Abrahão Dias[1] and Joice Panzarin Savietto[1]

Recent studies have provided information about digital eye strain and the potential damage that blue light from digital devices can cause to the eyes. In this study, we analyzed the influence of blue light exposure on reconstructed 3-dimensional skin model using RNA sequencing to identify the expression of transcripts and abnormal events. Three-dimensional skin was exposed to visible light spectrum and isolated blue wavelength for 1, 2, and 4 hours to represent acute exposure and 1 hour over 4 sequential days to represent repeated exposure, respectively, in this in vitro model. We compared gene expression levels with those of unexposed control. Samples submitted to repeated exposure showed reduced *AK2* and *DDX47*, whereas they showed increased *PABPC3* gene expression, revealing a significantly negative impact. RT-PCR validation assay with exposed 3-dimensional skin compared with unexposed control regarding 1 and 4 days of incubation showed increased IL-6 signaling mechanism activation and signal transducer and activator of transcription 3 gene *STAT3* gene expression, whereas it showed decreased peroxisome proliferator–activated receptor signaling mechanism activation, suggesting an influence on inflammatory pathways. We also demonstrate upregulated gene expression of *KIT*, *MAPK2*, and *PI3KC* in samples from exposed condition, corroborating previous findings related to pigmentation signaling stimuli. These results reveal, to our knowledge, previously unreported data that enable studies on molecular response correlation of in vitro digital blue light exposure and human skin studies.

Keywords: Methods/Tools/Techniques, Photobiology

JID Innovations (2024);**4:**100252 doi:10.1016/j.xjidi.2023.100252

INTRODUCTION

Blue wavelength light is part of the visible light spectrum and is referred to as high-energy visible light (Bernstein et al, 2021). The principal source of human exposure to blue light is the sun, although we receive a significant dose from electronic devices and indoor lighting (Bao et al, 2021), given a workday context of hours of exposure in front of computers and personal devices such as cellphones, television, etc.

Studies with blue light exposure have demonstrated evidence of eye damage (Marek et al, 2018; Vicente-Tejedor et al, 2018). On the other hand, blue light plays a critical role in the maintenance of health, being responsible for circadian cycle regulation in humans (Brown, 2020; Lawrenson et al, 2017; Tähkämö et al, 2019; Wahl et al, 2019). Blue light also increases humor and helps in cognitive functions and memory (Alkozei et al, 2017; Motamedzadeh et al, 2017). Regarding skin conditions, blue light can induce both beneficial and adverse effects, depending on the dose and the spectrum width of the exposure (Bonnans et al, 2020; Serrage et al, 2019).

Over the past several years, new evidence of blue light's contribution to effects on healthy human skin (Falcone et al, 2018), including hyperpigmentation (Campiche et al, 2020; Duteil et al, 2020; Regazzetti et al, 2018) has emerged, but it is still inconclusive whether this evidence can be generalized as a skin photoaging hazard, given no evidence of negative effects in real life (Ceresnie et al, 2023). Concerns about the harmful effects of blue light on the skin have increased, and knowledge about this topic is also increasing (Coats et al, 2021). For example, in 2010, a clinical study revealed that UVA and visible light could induce pigmentation in skin types IV–VI but not in light-skinned subjects, with different qualities and quantities of pigment (Mahmoud et al, 2010). In 2019, a study showed that epidermal skin cells could sense light and control their clock gene expression (Dong et al, 2019).

To properly study blue light effects on the skin, it is necessary to take both indoor and outdoor approaches because sunlight and digital devices emit blue light. Biological effects caused by blue light have been mapped (Kumari et al, 2023; Mahmoud et al, 2010; Regazzetti et al, 2018), although the nature of alterations in the biological

[1]*Natura Cosméticos S/A, São Paulo, Brazil*

Correspondence: Juliana Carvalhães Lago, Natura Cosméticos S/A, Via de Acesso, KM30,5, Prédio C - Cajamar – São Paulo CEP 07790-190, Brazil. E-mail: julianalago@natura.net

Abbreviations: 3D, 3-dimensional; LED, light-emitting diode; PPAR, peroxisome proliferator–activated receptor; RNA-seq, RNA next-generation sequencing

Received 13 December 2021; revised 9 November 2023; accepted 16 November 2023; accepted manuscript published online XXX; corrected proof published online XXX

Cite this article as: JID Innovations 2024;4:100252

mechanism remains unclear. Given its proximity to the UVA wavelength, studies suggest that blue light contributes to cutaneous alterations by ROS production, similar to UVA (Nakashima et al, 2017; Vandersee et al, 2015). Moreover, shorter wavelengths of visible light seem to induce long-lasting hyperpigmentation in melanocompetent individuals, mainly reported in melanocytes studies (Regazzetti et al, 2018). In contrast, information about longer blue wavelengths showed antifibrotic activity and may represent a suitable approach to treating fibrotic skin diseases (Krassovka et al, 2020).

Blue light–induced hyperpigmentation in dark-skinned subjects is known to be mediated by opsin 3 (Regazzetti et al, 2018); however, whether blue light also induces other molecular alterations in the skin is unknown. In this work, using next-generation sequencing (RNA-seq) and real time reverse transcriptase PCR (real time RT-PCR) validation, we identify biological pathways modulated differently during digital light exposure, including blue wavelength, suggesting a significantly negative impact on molecular events in a 3-dimensional (3D) skin model.

RESULTS AND DISCUSSION

We exposed 3D skin to 8 different conditions of light-emitting diode (LED) light exposure to simulate acute and repeated exposure. In addition, we compared the RNA-seq transcripts with those of unexposed 3D skin control to evaluate the role of blue wavelength on biological mechanisms of the skin, irradiated by visible light from a LED source in different exposure conditions.

Histological analysis

Samples from 8 groups of 3D skin, 3 replicates, irradiated using LED light and compared with unexposed control for 1 and 4 days of incubation were examined histologically. Three groups were simulating acute exposure (1, 2, and 4 hours), whereas the 3D skin samples irradiated for 1 hour over 4 sequential days were simulating repeated exposure for both blue wavelength and the full visible spectrum of digital light. Each sample of the replicate was analyzed within 10 histological sections, and Figure 1 represents a typical finding of the total number of replicates performed. The developed reconstructed 3D skin model exhibited high-quality histology and cytoarchitecture consistency. A critical hallmark of tridimensional skin maturation, including the dermis and epidermis, is the formation of the cornified envelope in the epidermis corneal layer (Sriram et al, 2018). As shown in Figure 1, all samples exhibited well-differentiated and multiple-layered epidermis. In addition, a well-differentiated collagen 1 matrix–based dermis with pattern morphology fibroblasts is shown. H&E staining displayed the characteristic basal columnar keratinocytes located at the basal layer and a visible stratum corneum. As a result, all 3D skin models demonstrated a high quality of the expected epidermal and dermal structure (Figure 1), suggesting that the biological difference associated with the transcript obtained in this study, when compared with those of unexposed control, is not directly related to morphological alterations on 3D skin.

RNA-seq and transcript analysis

The aging of the skin is a complex biological mechanism. The influence of the external environment is well-described in the literature (Lago and Puzzi, 2019). It is characterized by alterations in the physiology and morphology of the skin caused by sunlight exposure, yet little is known about the influence of digital light exposure on the skin. In this study, through RNA-seq and real-time RT-PCR validation, we evaluate the influence of blue wavelength and the full visible spectrum of digital light on skin biological mechanisms.

After isolation of total RNA, we performed RNA-seq assay (Gene Expression Omnibus identification GSE190106). Data analysis was performed using likelihood ratio test statistical method (Chen et al, 2020) in addition to Ingenuity Pathway Analysis software for pathway analysis. A representative image of differential gene expression in all digital light exposure models can be found in Figure 2a. The spectrum of colors indicates activation of the biological mechanism, with unexposed 3D skin being used as a control. For example, blue indicates downregulation of mechanism activation, whereas orange indicates upregulation.

Briefly, 8 groups of 3D skin samples were irradiated using LED light, and 3 replicates for each condition were pooled to identify the influence of digital blue light on skin biological mechanisms, compared with unexposed control (Table 1). Differential gene expression analysis was normalized using unexposed 3D skin as a control, for 1 day of incubation, and the pathway analysis was performed using Ingenuity Pathway Analysis software to determine the molecular damage caused in 3D skin exposed in each experimental condition (Supplementary Table S1). The heat map (Figure 2a) displays the z-scores from comparison analysis of canonical pathways activity (orange and blue rectangles). The z-score statistical method measures how close gene expression data in dataset compare with the pattern expected on the basis of the literature (Krämer et al, 2014).

One of the surprising findings of this study was that the 3D skin samples exposed to blue wavelength LED light in all 3 groups simulating acute exposure—1, 2, and 4 hours—exhibited mostly downregulation of mechanism activation, whereas the 3D skin samples irradiated for 1 hour over 4 sequential days simulating repeated exposure showed mostly upregulation of mechanism activation (Figure 2a and Supplementary Table S1). The same behavior was observed in samples exposed to the full visible spectrum (Figure 2a and Supplementary Table S1). Bonnans et al (2020) reported that blue light exposure could induce beneficial and adverse effects, depending on the dose, and the findings mentioned earlier suggest that continuous exposure to electronic devices emitting digital light can contribute to increasing molecular damage on skin biological mechanisms.

The impact of digital blue wavelength on repeated exposure conditions can be observed when we compare the same RNA-seq data obtained from blue wavelength exposure with data from full visible spectrum exposure (Figure 2b). The results from these 2 radiation conditions are similar, although with differing intensity of mechanism activation. Shorter-wavelength radiations are more energetic than longer ones, and blue wavelength ranges between approximately 400 and 500 nm (Bernstein et al, 2021). The skin samples directly

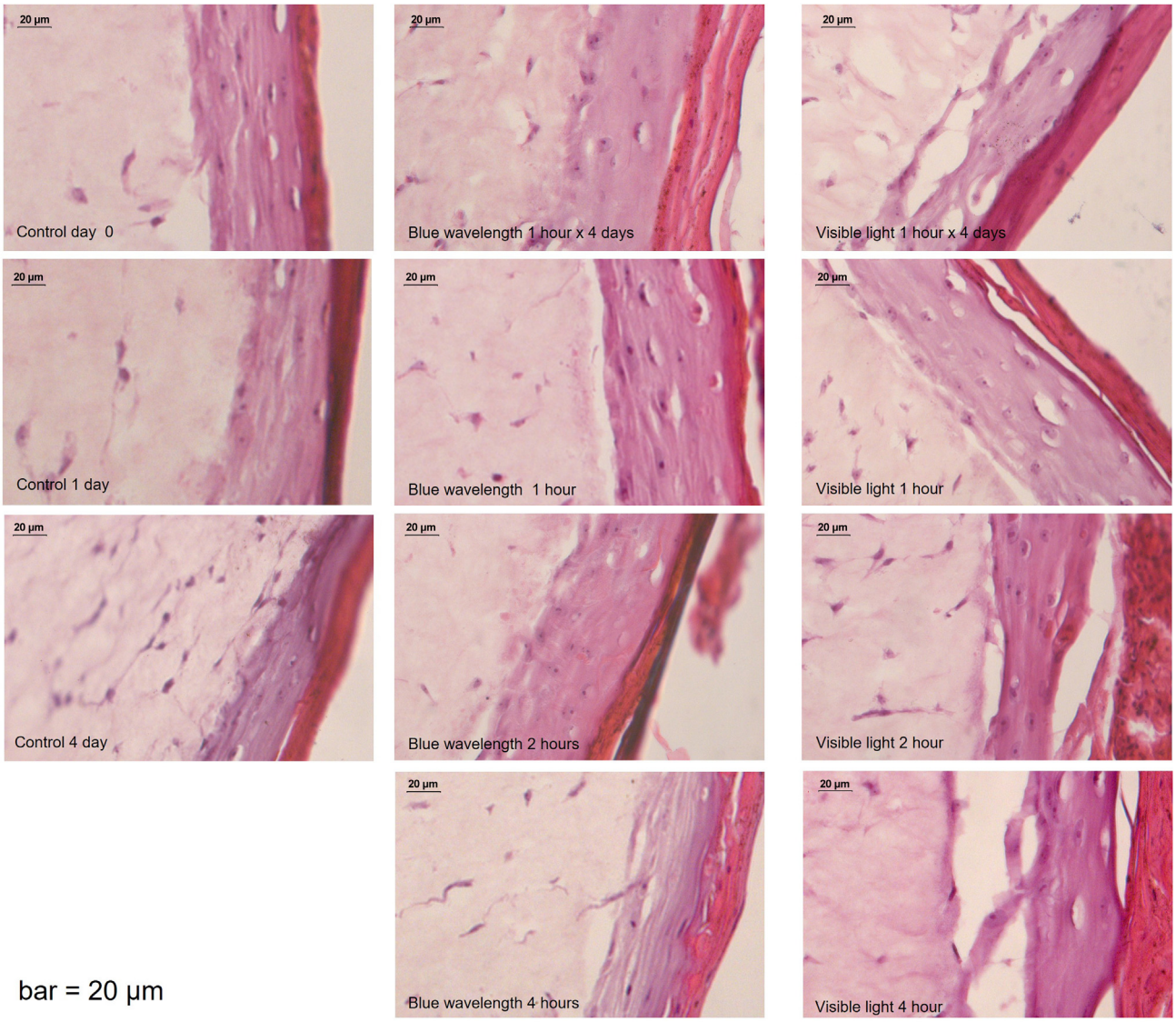

Figure 1. The 3D skin morphology analysis. H&E-stained cryopreserved sections of reconstructed 3D skin model are shown. Magnification = ×40. Comparison between samples simulating acute exposure (1, 2, and 4 h) and 1 group exposed for 1 h over 4 sequential days, simulating repeated exposure (1 h), both blue wavelength light and full visible light spectrum, was performed. In addition, 2 unexposed control samples with 1 and 4 days of incubation and 3 replicates were used. Each sample of the replicate was analyzed within 10 histological sections, and this figure represents a typical finding of the total number of replicates performed. All samples exhibited well-differentiated and multiple-layered epidermis and a well-differentiated collagen 1 matrix–based dermis with pattern morphology fibroblasts. H&E staining displayed the characteristic basal columnar keratinocytes located at the basal layer and a visible stratum corneum. 3D, 3-dimensional; h, hour.

exposed to blue wavelength light showed more intense damage than those exposed to the full visible spectrum. Observing the data, we can suggest that when skin is exposed to the full visible spectrum, the intensity of the high-energy visible wavelength is distributed over all the wavelengths and thereby diluted, which possibly decreases the ability to modulate but does not inhibit the gene expression.

Two additional experiments of RNA-seq assay were performed, and the tendency shown in the first experiment was confirmed (Gene Expression Omnibus identification GSE190106). In this study, 2 individual experiments with three 3D skin replicates were irradiated using LED light, for each condition pooled, and compared with unexposed control. Differentially expressed genes were defined as genes that were considered to have an increased or decreased expression when $P < .1$ and absolute values of $\log_2$ fold change > 0.4 were achieved in 1 or more treatments, relative to those of the unexposed control with 1 day of incubation. A 4-day incubation of unexposed control was included as a sample to evaluate the influence of incubation time progress. In this study, it was possible to observe reduced *AK2* gene expression of samples from 3D skin simulating repeated exposure compared with those of nonexposure 3D skin control (Figure 3a). *AK2* is critical to the control of energy metabolism, regulating intracellular adenosine triphosphate levels. Previous studies demonstrated that patients with no detectable AK2 protein demonstrated increased production of ROS and decreased adenosine triphosphate production (Ghaloul-Gonzalez et al, 2019), alterations well-described during aging as well (Sreedhar et al, 2020). Besides, the

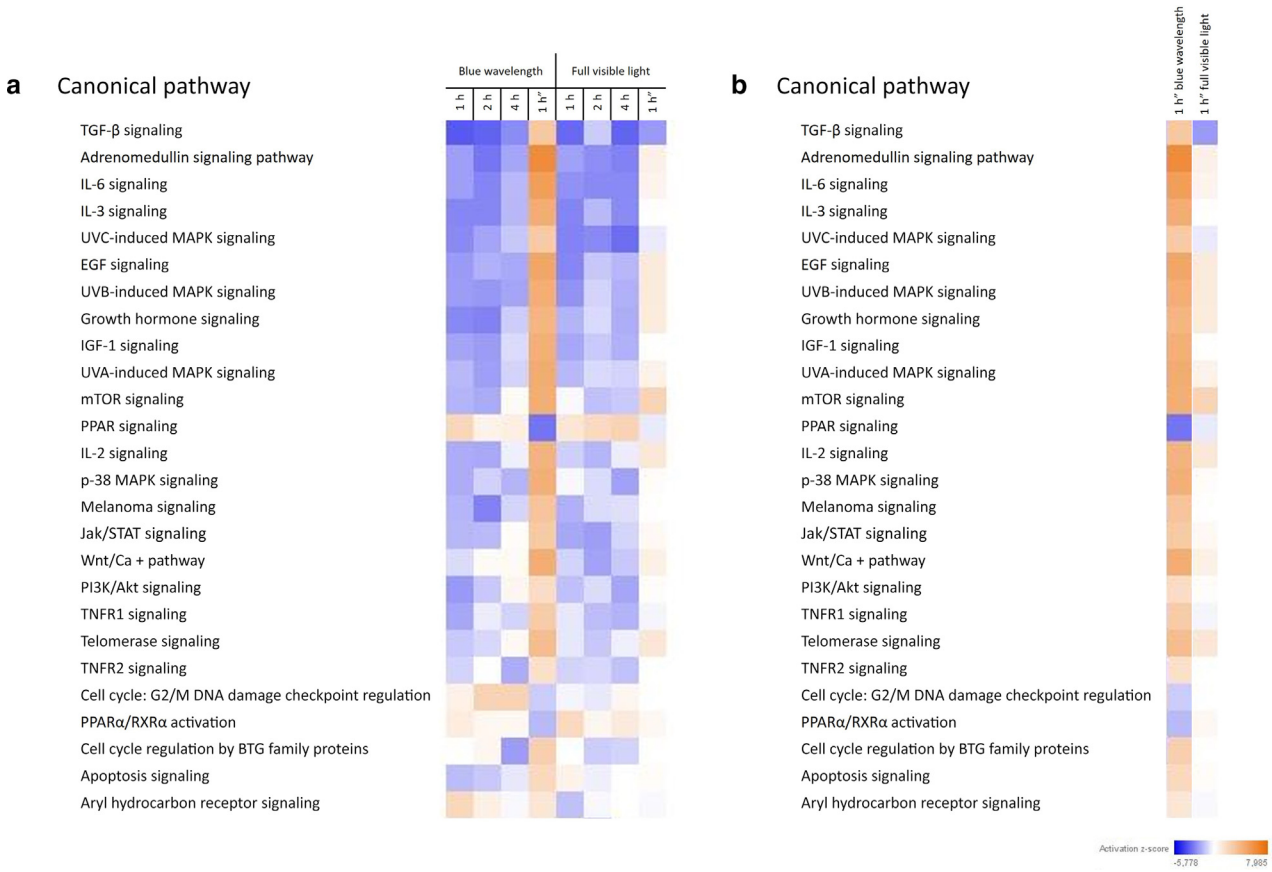

Figure 2. Comparison between samples exposed to both blue wavelength light and full visible light spectrum regarding differently modulated biological mechanisms; RNA-seq assay. Eight groups of 3D skin samples from experiment 1 were irradiated using LED light to identify the influence of digital light on 3D skin compared with unexposed control. (**a**) Three groups simulating acute exposure (1, 2, 4 h), whereas 1 group was exposed simulating repeated exposure (1 h), with both blue wavelength light and full visible light spectrum, regarding differently modulated biological mechanisms. (**b**) Samples simulating repeated exposure from experiment 1 of RNA-seq assay were compared regarding differently modulated biological mechanisms. Analysis of the activation of selected few pathways, with close relation with skin biological mechanisms, regarding z-score analysis. A complete table showing the values of z-scores from pathway activity analysis was added as Supplementary Table S1. The heat map displays the z-scores from pathway activity analysis: the blue color indicates downregulation of mechanism activation, whereas the orange color indicates upregulation. The z-score is a statistical method to measure how close gene expression data in a dataset compare with the pattern expected, on the basis of the literature. 3D, 3-dimensional; Akt, protein kinase B; h, hour; PI3K, phosphoinositide 3-kinase; PPAR, peroxisome proliferator–activated receptor; RNA-seq, RNA sequencing; STAT, signal transducer and activator of transcription.

gene expression of *DDX47*, whose encoded protein is believed to be involved in pre–ribosomal RNA processing and cell cycles pathway (Sekiguchi et al, 2006), is also reduced in samples from 3D skin simulating repeated exposure (Figure 3b).

Shen et al (2020) identified several novel genes, including *PABPC3*, mutated under different UVR conditions, suggesting that these genes are highly susceptible to UV-induced photodamage. Notably, our data reveal an increase of *PABPC3* gene expression ($\log_2$ fold change = 2.6, adjusted $P = 1.3e\text{-}04$) regarding samples of 3D skin simulating both acute and repeated exposure compared with that of nonexposed 3D skin control (Figure 3c). Taken together, these results provide potential means to study the correlation of molecular events in a 3D skin model and general damage to human skin in blue light–induced studies.

Real-time RT-PCR validation

To validate the findings, a real-time RT-PCR was performed comparing 3D skin samples irradiated with blue wavelength LED light for 1 hour over 4 sequential days, simulating repeated exposure, with unexposed controls regarding 1 and 4 days of incubation. Likewise, results exhibited upregulated mechanism activation of samples from repeated exposure compared with samples from both unexposed 3D skin controls (Figure 4). These data reinforce the initial observation, indicating that repeated exposure to digital blue light can play an essential role in enhancing the molecular damage caused to the skin, in agreement with previous data evidenced in recent studies (Mahmoud et al, 2010; Regazzetti et al, 2018).

The real-time RT-PCR assay was performed to validate blue wavelength–repeated exposure results. Two identical individual experiments were performed in 2 replicates, with three 3D skin replicates for each condition pooled. A total of 184 genes (Supplementary Table S2) were selected from RNA-seq assay after Ingenuity Pathway Analysis software analysis evaluation. We analyzed samples from 3D skin repeatedly exposed to blue wavelength LED light and 2 different conditions of nonexposure control, regarding 1 and 4 days of incubation, using TaqMan Array Fast 96-well Plate and 2(-Delta Delta C[T]) method (Livak and Schmittgen,

Table 1. Time of Exposure Using LED Light

Time		Blue Wavelength LED Light [lx]	Full Visible Spectrum LED Light [lx]	Mobile Phone Exposure [lx] (Reference)
Acute[1]	1 h	6,000 lm/m^2	5,880 lm/m^2	5100 lm/m^2
	2 h	12,000 lm/m^2	11,760 lm/m^2	10,200 lm/m^2
	4 h	24,000 lm/m^2	23,520 lm/m^2	20,400 lm/m^2
Repeated[2]	1 h × 4 d (1 h)	24,000 lm/m^2	23,520 lm/m^2	20,400 lm/m^2

Abbreviations: 3D, 3-dimensional; h, hour; LED, light-emitting diode.
[1]The 3D skin samples exposed to both blue wavelength light (400–450 nm) and full visible light spectrum (380–780 nm) simulating acute exposure.
[2]The 1, 2, and 4 h and 1 h over 4 sequential days simulating repeated exposure, all in 3 replicates. Illuminance is the total luminous flux incident on a surface per unit area. It has the lux (lx) as its unit of measurement, which is equal to 1 lumen per square meter (lm/m^2). Illuminance quantification was performed using a luxmeter.

2001) with *GAPDH* housekeeping gene used to calculate the relative fold gene expression of samples when performing real-time RT-PCR assay.

Concerning gene expression data, it is possible to observe differences in expression on the same gene by comparing these 2 experiments (Supplementary Table S2). The differences observed between experiments 1 and 2 are probably derived from individual response variations of the 3D skin samples. Although data from RNA transcripts are slightly different, the z-score statistics analysis demonstrated a similar activation of the mechanism. On the basis of this information, we can consider an equivalent response regarding molecular damage caused by blue light–induced exposure on 3D skin.

The samples from repeated exposure showed upregulated mechanism activation compared with those from unexposed 3D skin control with 1 and 4 days of incubation. The heat map (Figure 4) displays the z-scores from Pathway Activity Analysis. Blue indicates downregulation of mechanism activation, whereas orange indicates upregulation (Krämer et al, 2014).

Among many modulated biological mechanisms, we selected 3 Ingenuity Pathway Analysis canonical pathways to explore: IL-6 signaling, peroxisome proliferator–activated receptor (PPAR) signaling, and melanocyte development and pigmentation signaling. The inflammatory process is widely known as a premature skin aging signaling inductor (Pilkington et al, 2021). A consequence of this modulation can be hyperpigmentation (Mattos et al, 2017), a common symptom of aging skin (Choi et al, 2017; Lee, 2021; Ortonne, 1990). Therefore, we evaluated the gene expression behavior of pattern biomarkers for these mechanisms regarding transcript data.

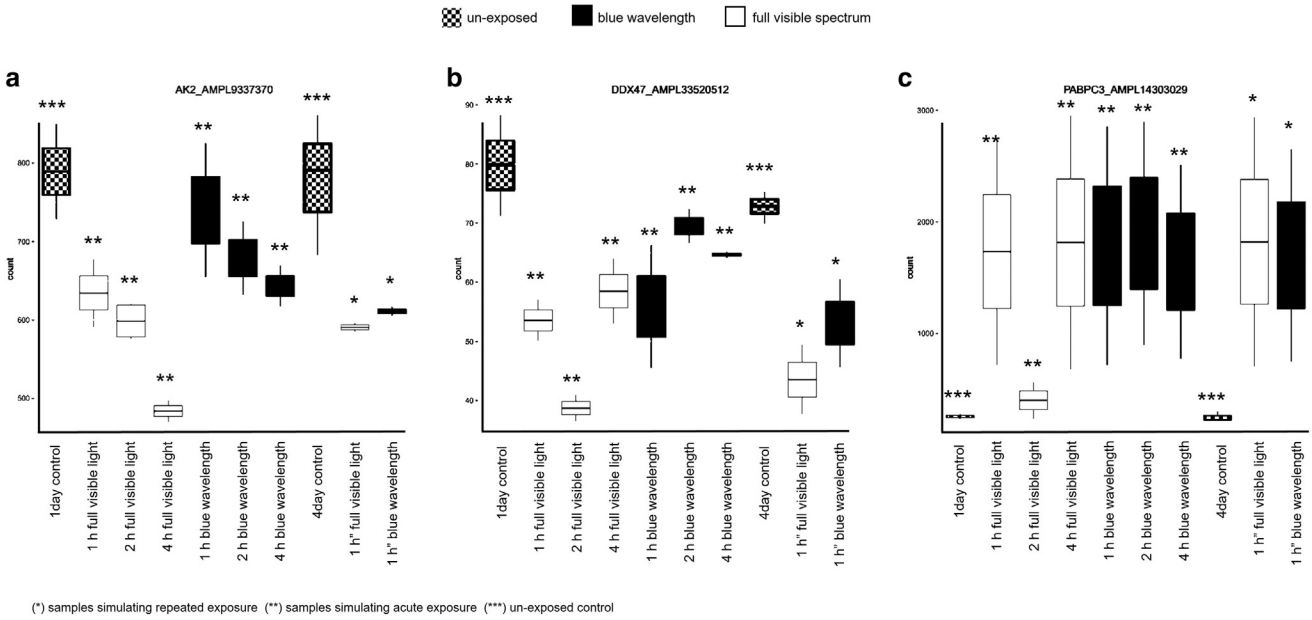

Figure 3. Comparison between samples exposed to both blue wavelength light and full visible light spectrum; RNA-seq assay. Samples simulating acute (1, 2, 4 h) and repeated exposure (1 h) from experiments 2 and 3 were compared and verified by Boxplot. DEGs are calculated as those with $P \leq .1$ and absolute values of log fold change ≥ 0.4. (**a**) Reduced *AK2* gene expression of samples from 3D skin simulating repeated exposure compared with that from nonexposed 3D skin control, regarding 1 and 4 days of incubation. (**b**) Reduced *DDX47* gene expression in samples from 3D skin simulating repeated exposure, compared with that in nonexposed 3D skin control, regarding 1 and 4 days of incubation. (**c**) Increase of *PABPC3* gene expression regarding samples of 3D skin simulating both acute and repeated exposure compared with that of nonexposed 3D skin control, regarding 1 and 4 days of incubation. The black, white, and checkered pattern boxes represent blue wavelength, full visible spectrum, and unexposed samples, respectively. The center line denotes the median value; the box contains the 25th–75th percentiles. The whiskers quartile ranges represent the minimum and maximum gene expression in each sample. 3D, 3-dimensional; DEG, differentially expressed gene; h, hour; RNA-seq, RNA sequencing. *Samples simulating repeated exposure; **samples simulating acute exposure; and ***un-exposed control.

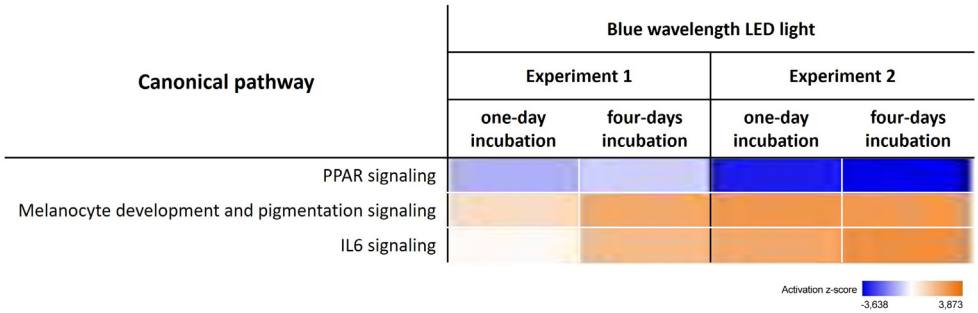

Figure 4. Comparison between samples exposed to blue wavelength LED light regarding IL-6 signaling, PPAR signaling, and melanocyte development and pigmentation signaling; real-time RT-PCR assay. Comparison between samples exposed for 1 h over 4 sequential days with blue wavelength light simulating repeated exposure (1 h), compared with nonexposure 3D skin control regarding 1 and 4 days of incubation was performed. Analysis of the activation of the mechanism regarding z-score analysis was conducted. The heat map displays the z-scores from pathway activity analysis: the blue color indicates downregulation of mechanism activation, whereas the orange color indicates upregulation. Only samples that reached the 1.3-fold upregulated or downregulated threshold were included for statistical analysis. The z-score is a statistical method to measure how close gene expression data in a dataset compare with the pattern expected, on the basis of the literature. 3D, 3-dimensional; h, hour; LED, light-emitting diode; PPAR, peroxisome proliferator–activated receptor.

IL-6 signaling. IL-6 is considered a regulator of the acute phase of inflammatory responses (Millrine et al, 2023; Xing et al, 1998). It is involved in the growth and differentiation of numerous cell types, and in the skin, it is critically involved in barrier repair after injury (Wang et al, 2004). In this study, we found gene expression related to IL-6 signaling differently modulated from unexposed samples. This signaling showed increased activation of the biological mechanism during repeated exposure condition. Observing IL-6 signaling mechanism activation on real-time RT-PCR validation assay for samples exposed to blue wavelength LED light, this signaling was upregulated in 3D skin samples simulating repeated exposure (Figure 4). Previous studies have shown that activation of IL-6 signaling increases signal transducer and activator of transcription 3 gene *STAT3* expression (Wang et al, 2004). In this study, it is possible to observe the increase of IL-6 signaling mechanism activation on 3D skin exposed to blue wavelength. Interestingly, the initiation of *IL6* and *IL6R* transcript synthesis occurred in exposed 3D skin, and the signal transducer and activator of transcription 3 gene *STAT3* expression was upregulated in all conditions (Supplementary Table S3), suggesting a possible feedback control and influence of IL-6 signaling (Figure 4).

PPAR signaling. The PPAR family consists of *PPARα*, *PPARδ*, and *PPARγ*. They act as ligand-activated transcriptional regulators (Adhikary et al, 2011; Sauer, 2015), and changes in the transcriptome indicate influence in cutaneous inflammatory signaling (Konger et al, 2021; Ramot et al, 2015). In this study, we found that gene expression profiles related to PPAR signaling (Supplementary Table S4), concerning 3D skin samples exposed to blue wavelength light, were differently modulated from unexposed samples. According to initial results and considering results from real-time RT-PCR validation assay, when individually observing PPAR signaling activation, 3D skin samples exposed to blue wavelength exhibited downregulation of mechanism activation compared with samples from unexposed 3D skin control (Figure 4). Furthermore, when compared with repeated exposure of 3D skin regarding blue wavelength, we identified downregulation of PPAR signaling activation, whereas we observed upregulation of IL-6 signaling activation. These results suggest an influence of inflammatory pathways of the skin on PPAR signaling, corroborating previous findings that PPARs appear to be essential for regulating skin inflammation, and the function is suppressed by cytokines (Ramot et al, 2015; Sauer, 2015).

Melanocyte development and pigmentation signaling. This biological pathway is regulated in large part by *MITF* activation, and its activity is controlled by 2 signaling pathways: melanocyte-stimulating hormone and KIT signaling pathways (Kawakami and Fisher, 2017; Phung et al, 2011; Wu et al, 2000). Furthermore, studies showed that stimulation of the *KIT* receptor tyrosine kinase activates *MAPK* and phosphatidylinositol 3-kinase gene *PI3K* pathways (Todd et al, 2014). In this study, according to real-time RT-PCR assay results, we demonstrate data related to gene expression upregulation of *KIT*, *MAPK2*, and *PI3KC* (Supplementary Table S5) in 3D skin samples from repeated exposure compared with samples from unexposed condition, corroborating the previous finding. These results suggest that repeated exposure to 3D skin, regarding blue wavelength LED light, can potentially explain the mechanistic process leading to an increased hyperpigmentation profile (Figure 4).

In conclusion, on the basis of the results of this study, we demonstrated that repeated exposure to LED light could represent a comparably adverse factor on molecular damage of skin biological mechanisms, influenced by blue wavelength. Gene expression levels in 3D skin were differently modulated during repeated exposure to LED light, represented by 4 consecutive days of 1-hour exposure. However, the biological difference associated with transcript was not directly related to morphological alterations on 3D skin. These findings suggest that this in vitro method can provide a potential means to correlate the molecular response of digital blue light–induced studies from LED light devices as well as a screening method for cosmetic formulations.

MATERIALS AND METHODS

Reconstructed 3D skin models

Primary cells were from Lonza (Normal Human Neonatal Dermal Fibroblasts – Catalog #: CC-2509 and Human Neonatal Epidermal

Keratinocytes, pooled − Catalog #: 00192906). The reconstructed skin was prepared in 2 steps. Briefly, the dermal compartment was prepared using rat tail type I collagen gel (Corning) and 1.5×10^5 primary human dermal fibroblasts per construct. After polymerizing the collagen gel for 2 hours, 2.5×10^5 primary human epidermal keratinocytes were seeded on top of each construct and kept submerged in RAFT: KGM-Gold Bullet Kit Medium (1:1) for 24 hours. The inserts were then raised and maintained at the air−liquid interface for 10 days for stratification of the skin. The 3D skin was maintained in a 5% carbon dioxide incubator with low humidity (~50%).

Exposure to blue wavelength and full spectrum of visible light

To demonstrate the potential influence of blue wavelength caused by digital exposure, the 3D skin was exposed to LED light, applying both blue wavelength and full visible light spectrum separately and using a dark box for radiation and a 100 W LED RGB spotlight, 20 cm from the light source. Illuminance quantification was performed using a luxmeter. Illuminance is the total luminous flux incident on a surface per unit area. It has the lux (lx) as its unit of measurement, which is equal to 1 lumen per square meter (l m/m^2).

In this study, 10 groups of 3D skin samples were defined: 3 groups of acute exposure and 1 group of repeated exposure with both blue wavelength light (400−450 nm) and full visible light spectrum, in addition to 2 unexposed control with 1- and 4-day incubation, respectively, all in triplicate, analyzed separately as shown in Table 1. After 10 days of stratification of the skin, the 3D skin was exposed to blue wavelength and a full visible light spectrum for 1, 2, and 4 hours to represent acute exposure and for 1 hour on 4 sequential days to represent repeated exposure, defined as the maximum period of exposure with gene expression alterations and no cell viability compromise. No temperature variation was observed inside the dark box during the exposure period. After performing the last exposure, the 3D skin was maintained in a 5% carbon dioxide and 37 °C incubator overnight before total RNA extraction.

Histological analysis

Samples from 8 groups of 3D skin, 3 replicates, irradiated using LED light and compared with unexposed control, regarding 1 and 4 days of incubation, were examined histologically. Each sample of the replicate was analyzed within 10 histological sections, and Figure 1 represents a typical finding of the total number of replicates performed. After LED light exposure, samples of 3D skin were frozen by cryopreservation. For morphological evaluation, preserved tissues from each group were sectioned and stained with H&E (Pedrosa et al, 2017) and then examined microscopically under a Zeiss Axioskop 40 FL microscope. All images of tissues were obtained using Zen blue 2.5 white. Magnification = ×40.

RNA-seq assay

Three individual experiments of RNA-seq assay were performed, and three 3D skin replicates were irradiated using LED light; each condition was pooled and compared with unexposed control. Differentially expressed genes were defined as genes that were considered to have an increased or decreased expression when $P < .1$ and absolute values of $\log_2$ fold change > 0.4 were achieved in 1 or more treatments, relative to the unexposed control regarding 1 and 4 days of incubation. According to the manufacturer's instructions, the total RNA from 3D skin was extracted using Mini kit PureLink Purific RNA 50 Preps (Invitrogen) (Rump et al, 2010). The RNA-seq analysis was performed using the next-generation sequencing platform (ION chef e ION5S) and specific reagents for RNA-seq assay (library construction protocol: A26325 Ion AmpliSeq Transcriptome Human Gene Expression Kit; Q32852 Qubit RNA high sensitivity, broad range and extended range Assay Kits; 468802 Ion Library TaqMan Quantitation Kit; A27759 ION 540 kit-Chef) and likelihood ratio test statistical method (Chen et al, 2020) while keeping 3D unexposed samples as a control (Figure 3).

Real-time RT-PCR validation

A real-time RT-PCR assay was performed to validate the results shown from the RNA-seq assay. Two individual experiments were performed in 2 replicates, with three 3D skin replicates for each condition pooled. We analyzed samples from 3D skin repeatedly exposed to blue wavelength LED light and 2 different conditions of nonexposure control, regarding 1 and 4 days of incubation. The total RNA from the 3D skin was extracted using the Mini Kit PureLink Purific RNA 50 Preps (Invitrogen) (Rump et al, 2010) according to the manufacturer's instructions. The cDNA was synthesized utilizing a High-Capacity cDNA Reverse Transcription Kit (Applied Biosystems), and a real-time RT-PCR analysis was performed according to the TaqMan protocol (Applied Biosystems) using TaqMan Array Fast, 96-well Plate, and Thermal Cycler StepOne (Thermo Fisher Scientific). Gene expression levels were estimated using ExpressionSuite software and 2(-Delta Delta C[T]) method for differential gene expression analysis (Livak and Schmittgen, 2001) with *GAPDH* housekeeping gene, using 3D skin unexposed samples as control (Supplementary Table S2).

Statistical analysis

The statistical comparisons between groups were performed by 2(-Delta Delta C[T]) method (Livak and Schmittgen, 2001) and likelihood ratio test statistical method (Chen et al, 2020). Differentially expressed gene analysis was performed using the Ion Torrent ampliSeqRNA plugin to alignment and raw read counts generation, followed by the R package DESeq2 (version 1.36.0) pipeline (Love et al, 2014). Genes with less than 10 normalized read counts were filtered out, and adjusted $P \leq .1$ and absolute values of $\log_2$ fold change ≥ 0.4 were used to screen for genes for RT-PCR validation. The likelihood ratio test was used to contrast conditions when testing all interactions together supplemented with Wald test when ignoring wavelength differences. Adjusted *P*-values were obtained using the Benjamini−Hochberg method implemented in DESeq2.

Comparison Analysis from Canonical Pathways was performed, and the heat map of the z-scores from pathway activity analysis was displayed (orange and blue rectangles). Only samples that reached the 1.3-fold upregulated or downregulated threshold were included for statistical analysis. Conceptually, the z-score statistical method measures how close gene expression data in dataset compare with the pattern expected, on the basis of the literature (Krämer et al, 2014).

DATA AVAILABILITY STATEMENT

The data discussed in this publication have been deposited to the National Center for Biotechnology Information's Gene Expression Omnibus (Edgar et al., 2002) and are accessible through Gene Expression Omnibus Series accession number GSE190106 (https://www.ncbi.nlm.nih.gov/geo/query/acc.cgi?acc=GSE190106).

ORCIDs

Juliana Carvalhães Lago: http://orcid.org/0000-0002-6383-8412
Ana Luisa Abrahão Dias: http://orcid.org/0000-0002-8698-4594

Melissa Dibbernn Ganzerla: http://orcid.org/0000-0001-8238-0809
Joice Panzarin Savietto: http://orcid.org/0000-0002-0706-8468

CONFLICT OF INTEREST

The authors state no conflict of interest.

ACKNOWLEDGMENTS

We thank Silvya Stuchi Maria Engler for 3-dimensional skin biofabrication and Lucas Pedersen Parizzi for statistics analysis. This work was funded by Natura Cosméticos S/A, a commercial cosmetic manufacturer. JCL, MDG, ALAD, and JPS were employees of Natura Cosméticos S/A at the time of the study and currently. JCL was directly involved in the design, implementation, analysis, and interpretation of the data.

AUTHOR CONTRIBUTIONS

Conceptualization: JCL, MDG, ALAD, JPS; Data Curation: JCL, ALAD; Formal Analysis: JCL; Funding Acquisition: JCL; Investigation: MDG, ALAD, JPS; Methodology: JCL; Project Administration: JCL; Resources: JCL, MDG, ALAD, JPS; Software: JCL; Supervision: JCL; Validation: JCL, ALAD; Visualization: JCL; Writing — Original Draft Preparation: JCL; Writing — Review and Editing: JCL, MDG, ALAD, JPS

SUPPLEMENTARY MATERIAL

Supplementary material is linked to the online version of the paper at www.jidonline.org, and at https://doi.org/10.1016/j.xjidi.2023.100252.

REFERENCES

Adhikary T, Kaddatz K, Finkernagel F, Schönbauer A, Meissner W, Scharfe M, et al. Genomewide analyses define different modes of transcriptional regulation by peroxisome proliferator-activated receptor-β/δ (PPARβ/δ). PLoS One 2011;6:e16344.

Alkozei A, Smith R, Dailey NS, Bajaj S, Killgore WDS. Acute exposure to blue wavelength light during memory consolidation improves verbal memory performance. PLoS One 2017;12:e0184884.

Bao J, Song X, Li Y, Bai Y, Zhou Q. Effect of lighting illuminance and colour temperature on mental workload in an office setting. Sci Rep 2021;11:15284.

Bernstein EF, Sarkas HW, Boland P. Iron oxides in novel skin care formulations attenuate blue light for enhanced protection against skin damage. J Cosmet Dermatol 2021;20:532–7.

Bonnans M, Fouque L, Pelletier M, Chabert R, Pinacolo S, Restellini L, et al. Blue light: friend or foe. J Photochem Photobiol B 2020;212:112026.

Brown TM. Melanopic illuminance defines the magnitude of human circadian light responses under a wide range of conditions. J Pineal Res 2020;69:e12655.

Campiche R, Curpen SJ, Lutchmanen-Kolanthan V, Gougeon S, Cherel M, Laurent G, et al. Pigmentation effects of blue light irradiation on skin and how to protect against them. Int J Cosmet Sci 2020;42:399–406.

Ceresnie MS, Patel J, Lim HW, Kohli I. The cutaneous effects of blue light from electronic devices: a systematic review with health hazard identification. Photochem Photobiol Sci 2023;22:457–64.

Chen Y, Moustaki I, Zhang H. A note on likelihood ratio tests for models with latent variables. Psychometrika 2020;85:996–1012.

Choi W, Yin L, Smuda C, Batzer J, Hearing VJ, Kolbe L. Molecular and histological characterization of age spots. Exp Dermatol 2017;26:242–8.

Coats JG, Maktabi B, Abou-Dahech MS, Baki G. Blue light protection, part I-effects of blue light on the skin. J Cosmet Dermatol 2021;20:714–7.

Dong K, Goyarts EC, Pelle E, Trivero J, Pernodet N. Blue light disrupts the circadian rhythm and create damage in skin cells. Int J Cosmet Sci 2019;41:558–62.

Duteil L, Queille-Roussel C, Lacour JP, Montaudié H, Passeron T. Short-term exposure to blue light emitted by electronic devices does not worsen melasma. J Am Acad Dermatol 2020;83:913–4.

Edgar R, Domrachev M, Lash AE. Gene expression omnibus: NCBI gene expression and hybridization array data repository. Nucleic Acids Res 2002;30:207–10.

Falcone D, Uzunbajakava NE, van Abeelen F, Oversluizen G, Peppelman M, van Erp PEJ, et al. Effects of blue light on inflammation and skin barrier recovery following acute perturbation. Pilot study results in healthy human subjects. Photodermatol Photoimmunol Photomed 2018;34:184–93.

Ghaloul-Gonzalez L, Mohsen AW, Karunanidhi A, Seminotti B, Chong H, Madan-Khetarpal S, et al. Reticular dysgenesis and mitochondriopathy induced by adenylate kinase 2 deficiency with atypical presentation. Sci Rep 2019;9:15739.

Kawakami A, Fisher DE. The master role of microphthalmia-associated transcription factor in melanocyte and melanoma biology. Lab Invest 2017;97:649–56.

Konger RL, Derr-Yellin E, Zimmers TA, Katona T, Xuei X, Liu Y, et al. Epidermal PPARγ is a key homeostatic regulator of cutaneous inflammation and barrier function in mouse skin. Int J Mol Sci 2021;22:8634.

Krämer A, Green J, JJr Pollard, Tugendreich S. Causal analysis approaches in Ingenuity Pathway Analysis. Bioinformatics 2014;30:523–30.

Krassovka JM, Suschek CV, Prost M, Grotheer V, Schiefer JL, Demir E, et al. The impact of non-toxic blue light (453 nm) on cellular antioxidative capacity, TGF-β1 signaling, and myofibrogenesis of human skin fibroblasts. J Photochem Photobiol B 2020;209:111952.

Kumari J, Das K, Babaei M, Rokni GR, Goldust M. The impact of blue light and digital screens on the skin. J Cosmet Dermatol 2023;22:1185–90.

Lago JC, Puzzi MB. The effect of aging in primary human dermal fibroblasts. PLoS One 2019;14:e0219165.

Lawrenson JG, Hull CC, Downie LE. The effect of blue-light blocking spectacle lenses on visual performance, macular health and the sleep-wake cycle: a systematic review of the literature. Ophthalmic Physiol Opt 2017;37:644–54.

Lee AY. Skin pigmentation abnormalities and their possible relationship with skin aging. Int J Mol Sci 2021;22:3727.

Livak KJ, Schmittgen TD. Analysis of relative gene expression data using real-time quantitative PCR and the 2(-Delta Delta C(T)) method. Methods 2001;25:402–8.

Love MI, Huber W, Anders S. Moderated estimation of fold change and dispersion for RNA-seq data with DESeq2. Genome Biol 2014;15:550.

Mahmoud BH, Ruvolo E, Hexsel CL, Liu Y, Owen MR, Kollias N, et al. Impact of long-wavelength UVA and visible light on melanocompetent skin. J Invest Dermatol 2010;130:2092–7.

Marek V, Mélik-Parsadaniantz S, Villette T, Montoya F, Baudouin C, Brignole-Baudouin F, et al. Blue light phototoxicity toward human corneal and conjunctival epithelial cells in basal and hyperosmolar conditions. Free Radic Biol Med 2018;126:27–40.

Mattos KPH, Cintra ML, Gouvêa IR, Ferreira LÁ, Velho PENF, Moriel P. Skin hyperpigmentation following intravenous polymyxin B treatment associated with melanocyte activation and inflammatory process. J Clin Pharm Ther 2017;42:573–8.

Millrine D, Cardus Figueras A, Uceda Fernandez J, Andrews R, Szomolay B, Cossins BC, et al. Th1 cells alter the inflammatory signature of IL-6 by channeling STAT transcription factors to Alu-like retroelements. J Immunol 2023;211:274–86.

Motamedzadeh M, Golmohammadi R, Kazemi R, Heidarimoghadam R. The effect of blue-enriched white light on cognitive performances and sleepiness of night-shift workers: a field study. Physiol Behav 2017;177:208–14.

Nakashima Y, Ohta S, Wolf AM. Blue light-induced oxidative stress in live skin. Free Radic Biol Med 2017;108:300–10.

Ortonne JP. The effects of ultraviolet exposure on skin melanin pigmentation. J Int Med Res 1990;18:8C–17C.

Pedrosa TDN, Catarino CM, Pennacchi PC, Assis SR, Gimenes F, Consolaro MEL, et al. A new reconstructed human epidermis for in vitro skin irritation testing. Toxicol In Vitro 2017;42:31–7.

Phung B, Sun J, Schepsky A, Steingrimsson E, Rönnstrand L. C-KIT signaling depends on microphthalmia-associated transcription factor for effects on cell proliferation. PLoS One 2011;6:e24064.

Pilkington SM, Bulfone-Paus S, Griffiths CEM, Watson REB. Inflammaging and the skin. J Invest Dermatol 2021;141:1087–95.

Ramot Y, Mastrofrancesco A, Camera E, Desreumaux P, Paus R, Picardo M. The role of PPARγ-mediated signalling in skin biology and pathology: new targets and opportunities for clinical dermatology. Exp Dermatol 2015;24:245–51.

Regazzetti C, Sormani L, Debayle D, Bernerd F, Tulic MK, De Donatis GM, et al. Melanocytes sense blue light and regulate pigmentation through Opsin-3. J Invest Dermatol 2018;138:171–8.

Rump LV, Asamoah B, Gonzalez-Escalona N. Comparison of commercial RNA extraction kits for preparation of DNA-free total RNA from Salmonella cells. BMC Res Notes 2010;3:211.

Sauer S. Ligands for the nuclear peroxisome proliferator-activated receptor gamma [published correction appears in Trends Pharmacol Sci 2016;37:167] Trends Pharmacol Sci 2015;36:688–704.

Sekiguchi T, Hayano T, Yanagida M, Takahashi N, Nishimoto T. NOP132 is required for proper nucleolus localization of DEAD-box RNA helicase DDX47. Nucleic Acids Res 2006;34:4593–608.

Serrage H, Heiskanen V, Palin WM, Cooper PR, Milward MR, Hadis M, et al. Under the spotlight: mechanisms of photobiomodulation concentrating on blue and green light. Photochem Photobiol Sci 2019;18:1877–909.

Shen Y, Ha W, Zeng W, Queen D, Liu L. Exome sequencing identifies novel mutation signatures of UV radiation and trichostatin A in primary human keratinocytes. Sci Rep 2020;10:4943.

Sreedhar A, Aguilera-Aguirre L, Singh KK. Mitochondria in skin health, aging, and disease. Cell Death Dis 2020;11:444.

Sriram G, Alberti M, Dancik Y, Wu B, Wu R, Feng Z, et al. Full-thickness human skin-on-chip with enhanced epidermal morphogenesis and barrier function. Mater Today 2018;21:326–40.

Tähkämö L, Partonen T, Pesonen AK. Systematic review of light exposure impact on human circadian rhythm. Chronobiol Int 2019;36:151–70.

Todd JR, Scurr LL, Becker TM, Kefford RF, Rizos H. The MAPK pathway functions as a redundant survival signal that reinforces the PI3K cascade in c-Kit mutant melanoma. Oncogene 2014;33:236–45.

Vandersee S, Beyer M, Lademann J, Darvin ME. Blue-violet light irradiation dose dependently decreases carotenoids in human skin, which indicates the generation of free radicals. Oxid Med Cell Longev 2015;2015:579675.

Vicente-Tejedor J, Marchena M, Ramírez L, García-Ayuso D, Gómez-Vicente V, Sánchez-Ramos C, et al. Removal of the blue component of light significantly decreases retinal damage after high intensity exposure. PLoS One 2018;13:e0194218.

Wahl S, Engelhardt M, Schaupp P, Lappe C, Ivanov IV. The inner clock-Blue light sets the human rhythm. J Biophotonics 2019;12:e201900102.

Wang XP, Schunck M, Kallen KJ, Neumann C, Trautwein C, Rose-John S, et al. The interleukin-6 cytokine system regulates epidermal permeability barrier homeostasis. J Invest Dermatol 2004;123:124–31.

Wu M, Hemesath TJ, Takemoto CM, Horstmann MA, Wells AG, Price ER, et al. c-kit triggers dual phosphorylations, which couple activation and degradation of the essential melanocyte factor Mi. Genes Dev 2000;14:301–12.

Xing Z, Gauldie J, Cox G, Baumann H, Jordana M, Lei XF, et al. IL-6 is an antiinflammatory cytokine required for controlling local or systemic acute inflammatory responses. J Clin Invest 1998;101:311–20.